ELSEVIER

Coordination Chemistry Reviews
147 (1996) 87–115

COORDINATION CHEMISTRY REVIEWS

Effective core potential studies of transition metal bonding, structure and reactivity

Mark S. Gordon [a], Thomas R. Cundari [b]

[a] *Department of Chemistry, Iowa State University, Ames, IA 50011, USA*
[b] *Department of Chemistry, University of Memphis, Memphis, TN 38152, USA*

Received 20 May 1994

Contents

Abstract

Computational methods for the analysis of transition metal complexes have undergone rapid progress in the recent past. Improved methods, most notably effective core potentials including relativistic correlations, new methods for determining analytic first and second energy derivatives and efficient methods for obtaining multiconfiguration wavefunctions, have been developed. Combined with new computational technologies, most notably the development of parallel hardware and software, this provides exciting new opportunities to investigate quantitatively the bonding, structure and reactivity of complexes incorporating transition metals from the entire series. This review covers recent work from our laboratories, in which all of these emerging technologies have been used. Subjects to be discussed include the nature of multiple bonds between transition metals and main group elements and the activation of prototypical bonds by transition metals.

We focus on multiply bonded transition metal–main group (TM=MG) complexes of the early transition metals, because of the vigorous experimental research that has been done in this area, particularly as it pertains to catalysis and advanced materials applications. The bonding and structure of alkylidene ($L_nM{=}C(R)R'$), silylidene ($L_nM{=}Si(R)R'$) and imido

SSDI 0010-8545(95)01133-1

($L_nM{=}NR$) complexes are reviewed. Some recent results on oxo ($L_nM{=}O$), sulfido ($L_nM{=}S$) and phosphinidine ($L_nM{=}PR$) complexes are also presented. Bonding is, in general, interpreted using the language of valence bond theory, made possible by the development of localization methods for multiconfigurational orbitals. This approach is quite useful, since it conforms to the language used by the experimental community in their analyses of the bonding and reactivity of TM=MG complexes, yet it retains the fundamental molecular orbital approach. Of particular interest are the following questions.

(1) Can a computational scheme be developed to predict accurately the properties of experimentally characterized TM=MG species, thus allowing confidence in studies of TM=MG complexes whose reactivity is not conducive to X-ray structural analysis?

(2) For a given L_nM, how does the basic picture of metal–ligand multiple bonding change from alkylidene to imido to oxo, and from silylidene to phosphinidene to sulfido?

(3) What are the essential features of the potential energy surfaces relating to bond activation?

(4) How do TM=MG species involving the heavier elements (MG ≡ Si, P and S) compare with their lighter congeners?

(5) Are any trends in the properties of the transition metal–main group linkage discernible (as a function of M, L_n or E), which may provide new insight into the reactivity of these complexes in the various important processes in which they participate, and which may help to design more effective TM=MG materials through modification of the chemical environment?

Keywords: Core potential studies; Transition metals

1. Introduction

The transition metals (TMs) constitute a family of elements of obvious importance in fields such as advanced materials, catalysis and biochemistry [1]. Coordination chemistry owes its richness to the amazing ability of TMs to stabilize a variety of geometries, spin and oxidation states and ligand types, properties which are largely responsible for their utility in these technologically important areas. However, these properties, as well as others (e.g. the large number of low-energy excited states and the large size of many TM complexes), contribute to the many difficulties encountered in treating TMs using computational chemistry techniques. It is perhaps no accident that two recent compendia of research in this area contain the word "challenge" in their titles [2]. To meet the challenges of TM chemistry, a wide variety of computational approaches have been employed, and a review of computational TM chemistry has recently appeared in this journal [3].

As the impressive body of literature on ab initio studies of organic chemistry clearly demonstrates, ab initio methods have the potential to provide a quantitative prediction of geometries, reaction enthalpies, activation barriers and bond energies [4]. Computational TM chemistry has not yet progressed to the extent attained by computational organic chemistry, but because of the fundamental importance of the TMs in many areas of chemistry, this field continues to be one of major activity [2,5]. The recent dramatic improvements in computational methods and technology promise to propel computational TM chemistry to a level comparable with that of the lighter main group (MG) elements. The present contribution presents some of

the approaches to the challenges of coordination chemistry, as well as some of the results that have been obtained in our laboratories.

2. Nature of the problem

Three main challenges face the computational chemist with an interest in TM coordination chemistry [2]. First, the large number of electrons and orbitals which need to be described in the TMs, particularly those of the second and third row, have made all-electron studies of these systems computationally prohibitive in many circumstances. It is important to remember that the computational effort in Hartree–Fock, ab initio methods is roughly proportional to N^4, where N is the number of atomic orbitals (basis functions) which are needed to describe the system. Second, relativistic effects increase in significance as one descends to the heavier elements in the Periodic Table, and any credible model must treat these effects adequately. A third challenge in computational TM chemistry arises from the frequent existence of a large number of low-lying electronic states. This precludes the simple description of TM systems in terms of a single electronic configuration, and requires a multiconfigurational description as a starting point for the calculation. Related to this is the electron correlation problem that arises from the neglect of instantaneous electron–electron repulsions in the standard Hartree–Fock molecular orbital scheme (which forms the basis of the majority of quantum chemical methods). When it is necessary to include electron correlation (essential for the prediction of accurate energetics, and frequently necessary for the prediction of accurate TM=MG geometries), the computational effort can be proportional to N^5–N^7, potentially further limiting the size (and thus to some extent the experimental relevance) of systems which can be treated.

Our main algorithmic approach to the challenges of the TMs (and their lanthanide counterparts) incorporates the development and utilization of effective core potential (ECP) methods [6], in which inner shell electrons are replaced by a model potential. Combined with the use of reliable valence basis sets, modern techniques for treating electron correlation and emerging technologies such as parallel computing (the distribution of a single calculation over multiple processors), this appears to be a very powerful method for dealing with TM systems. This paper presents a summary of our research that has used this combination of methods as a tool to probe TM bonding and reactivity. The utility of ECPs, combined with modern computational techniques, is highlighted by focusing on a variety of recent applications.

This paper is organized in the following fashion. First, we start with a brief overview of the main computational methods used. This is followed by a discussion of several applications of these methods to the molecular and electronic structure and reactivity of TM complexes. Since TM=MG multiple bonding has been extensively studied by our groups, this work receives special consideration. The amazing reactivity of TM complexes has made them popular subjects for both experimental and theoretical chemical researchers, so that in the final section we review some of our work in this area, focusing on methane C–H activation.

3. Computational methods

An ECP is simply a group of potential functions (ideally a very small set) which replaces the core electron and core orbitals which are normally assumed to have a minor effect on most chemical phenomena [6]. The ECPs have the functional form shown in Eq. (1)

$$r^2 V_l(r) = \sum_k A_{l,k} r^{n_{l,k}} \exp(-B_{l,k} r^2) \quad (1)$$

Coefficients ($A_{l,k}$), radial exponents ($n_{l,k}$) and gaussian exponents ($B_{l,k}$) describe the radial extent and shape of the model potential. Basis sets for describing the valence electrons are of the familiar gaussian variety. Our groups have employed the ECPs and attendant valence basis sets (VBSs) of Stevens, Basch, Krauss and Jasien (SBKJ) [6a,b] which are built into the GAMES quantum chemistry program package [7]. The SBKJ scheme has been derived with an eye towards minimizing the number of terms needed in Eq. (1) to describe the potential generated by the core electrons; thus they are sometimes referred to as compact effective potentials (CEPs). ECPs and VBSs for TMs have been derived by other workers [6], most notably Hay and Wadt (HW) [6d], and used to good effect by various researchers [2,3,5,6].

Apart from the computational benefits outlined above, ECPs offer exciting "chemical" benefits for the coordination chemist. Since only valence electrons are treated, the computational effort remains the same for complexes which differ only in the central TM atom, regardless of its position in the transition series. With ECPs, a computational investigation of an Hf catalyst or advanced material precursor can be carried out with the same facility as studies of the Zr and Ti analogs. This allows the computational chemist to approach TM bonding and reactivity in the manner long employed by experimentalists, i.e. studying trends for related complexes, e.g. those congeners within a triad.

The calculations described below employ the computational chemistry program GAMESS [7] running on sequential, parallel and vector platforms. The ECPs and VBSs of SBKJ [6a,b] are used for heavy atoms, and the −31G basis set is used for H. ECPs replace the innermost core orbitals for the TMs and all core orbitals for MG elements. Thus the ns, np, nd, (n + 1)s and (n + 1)p are treated explicitly for the d block; for the MG, ns and np are treated explicitly [6a,b]. In the standard implementation, TM VBSs are quadruple and triple zeta for the sp and d shells respectively, while MG elements have a double-zeta valence basis [6a,b]. Basis sets for heavy MG elements are augmented with a d polarization function [4]. Unless otherwise stated, geometries are optimized at the restricted Hartree–Fock (RHF) level for closed shell singlets. Vibrational frequencies are always calculated at stationary points to identify them as minima (zero imaginary frequencies), transition states (one imaginary frequency) or higher order saddle points (two or more imaginary frequencies).

For coordinatively unsaturated systems and systems with weak TM−MG bonding (typically when MG is a third row element such as Si), one must often go beyond a single determinant description (vide infra) for even a qualitative understanding of the bonding in these complexes.

Although geometries are usually accurately predicted at the RHF level, energetics are expected to be poor if correlation is ignored. For species described well at the RHF level, the correlation contribution is a perturbation to the RHF energy, and can be calculated using many body perturbation theory. Typically, our choice has been the efficient second-order Moller–Plesset perturbation theory (MP2) [8]. An [RHF geometry/MP2 energy] scheme has been shown in our laboratories to yield good agreement with experimental data for processes such as methane elimination from d^0 methyl(amido) complexes of the Ti and V triad [9]. Calculated data are corrected for zero point energies and from absolute zero to experimentally relevant temperatures using RHF frequencies. In those cases for which a multiconfigurational self-consistent field (MCSCF) wavefunction is required for a qualitatively correct description of the molecular and electronic structure, the MCSCF wavefunction is augmented by either multireference configuration interaction (MRCI) [10] or multireference perturbation theory [11].

A particularly useful means for analyzing the nature of TM=MG multiple bonds combines simple MCSCF wavefunctions with the concept of localized molecular orbitals (LMOs), in order to provide a bridge between these complex ab initio calculations and a simple valence bond view of bonding. Let us consider the application of this MCSCF/LMO/CI approach to a prototypical TM=MG (M=E) double bond. A simple RHF description of a simple double bond is represented by the wavefunction

$$\Psi_{RHF} = |\ldots \sigma_{ME}{}^2 \pi_{ME}{}^2 (\pi_{ME}{}^*)^0 (\sigma_{ME}{}^*)^0|$$

so that the σ and π bonding orbitals for the ME bond are both doubly occupied and the corresponding antibonding orbitals are empty. A simple MCSCF wavefunction for this bond, referred to as MCSCF(4,4), includes all electronic configurations in which the four (σ and π) electrons in the bond are distributed among the four (bonding and antibonding) orbitals, giving rise to 20 electronic configurations. The more important the additional configurations become, the less correct it becomes to describe the electronic wavefunction simply by the closed shell, single determinant Hartree–Fock wavefunction Ψ_{RHF}. The importance of the additional configurations is easily assessed by diagonalizing the first-order density matrix for the MCSCF(4,4) wavefunctions. The eigenfunctions of the density matrix, the natural orbitals, will have occupation numbers near 2.0 for bonding and 0.0 for antibonding orbitals if the closed shell Hartree–Fock description is essentially correct. The more important a multiconfigurational description becomes, the larger the occupation numbers for the antibonding natural orbitals. Correspondingly, the occupation of the bonding orbitals decreases.

The MCSCF/LMO/CI procedure consists of three steps. In step 1, the MCSCF(4,4) wavefunction described above, consisting of 20 configurations, is generated. In step 2, the MCSCF natural orbitals are localized to yield "atomic orbital (AO)-like" molecular orbitals (MOs). These will correspond to σ_E, π_E, π_M, σ_M. The AO-like MOs are predominantly (more than 90%) located on either the TM (M) or MG (E) end of the ME bond. In step 3, a CI wavefunction consisting of the AO-like

MO active space is used to generate 20 configurations that now look like valence bond resonance structures and give the weight of each in the overall wavefunction. Generally, only a subset of these 20 configurations is chemically sensible. We denote the resonance structures as $|\sigma_E^a \pi_E^b \pi_M^c \sigma_M^d\rangle$, where a, b, c and d are the occupation numbers of the AO-like MOs. It is sensible to expect that those resonance structures which possess two electrons each in the σ and π manifolds (i.e. $a+d=2$; $b+c=2$) will be the primary contributors, since the compound thereby avoids large contributions from configurations with weaker one- or three-electron bonds.

4. Transition metal–ligand multiple bonding

Coordination compounds with multiple bonds between TMs and MG elements (TM=MG) have come under intense experimental scrutiny [12] because of their interesting structure and reactivity. Multiply bonded complexes are putative intermediates in a variety of industrial (e.g. imido complexes (L_nM=NR) in the ammoxidation of propylene), biological (e.g. oxo complexes (L_nM=O) in the cytochrome P-450-catalyzed oxidation of xenobiotics) and academic (e.g. carbene complexes (L_nM=C(R)R′) in organic synthesis) processes [12]. Complexes involving multiple bonds between TMs and the heavier MG elements (e.g. P, Si and S) are comparatively rare, although a growing number of examples have recently been reported [13]. Our initial studies of ECP methods focused on the fundamental nature of the bonding in TM=MG complexes, and its response to the chemical environment [9,14].

The essential features of a chemical reaction mechanism are contained in the minimum energy path(s) (MEP(s)) — the path(s) of steepest descent connecting reactants and products via transition states. A schematic of such an MEP (also referred to as an intrinsic reaction coordinate or IRC) is shown in Fig. 1, where the energy (ordinate) is plotted against the "reaction coordinate" s (abscissa). The coordi-

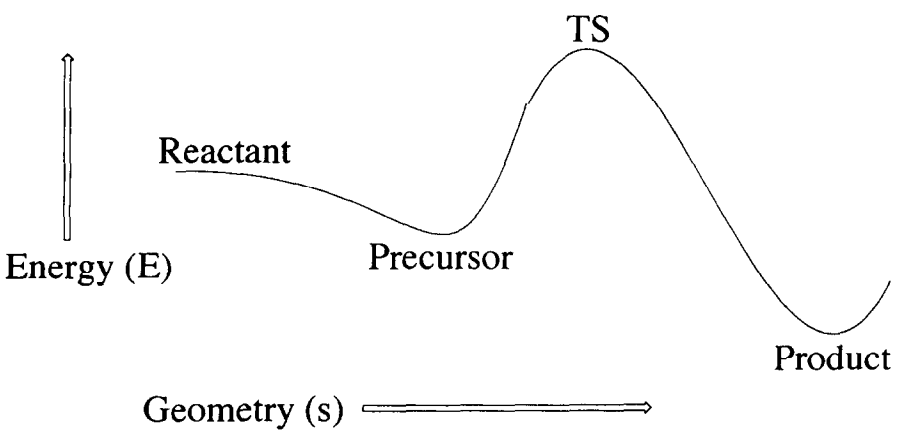

Fig. 1. Hypothetical reaction coordinate.

nate s represents a composite change in all geometric parameters (angles and bond lengths) as the reaction proceeds. To understand fully a reaction mechanism, experimentally or computationally, one first needs to characterize all of the stationary points (minima and transition states) along the MEP. This entails the evaluation of both the energy and the geometry at these stationary points, as well as an analysis of the bonding. Frequently, even this information is insufficient to understand fully the dynamics and kinetics of reaction mechanisms, and geometries and energies along the reaction path connecting the stationary points must also be probed. The following sections are organized to emphasize the appropriate level of treatment needed to carry out the tasks of describing the bonding, geometry and energetics of TM-containing systems in key regions of a reaction path.

4.1. Geometries

Generally, the first task in any computational study is to predict the geometry of stationary points on the potential energy surface of interest. Since it is important to calibrate the predictive ability of the computational method(s) being used, it is necessary to compare predicted geometries with experimental results when the latter are available. It is also essential to verify that predicted geometries correspond to potential energy minima (or transition states where appropriate) by calculating the matrix of energy second derivatives (hessian) and then diagonalizing that matrix. The existence of zero (one) negative eigenvalues shows that the corresponding geometry is a minimum (transition state) at that level of theory. The ECP scheme of SBKJ [6a,b] has performed extremely well with respect to the calculation of the geometries of TM=MG complexes [9,14]. In general, bond lengths and bond angles are predicted to within 3% of the experimental models, as long as a suitable level of theory is employed. Representative examples are given below and many more can be found in the original papers [9,14]. The ability of a computational scheme to predict accurately the geometry of many TM complexes gives confidence in structural predictions for species for which there is limited experimental data (e.g. reactive intermediates in a catalytic cycle), and it is a strong indication that the electronic structure of these complexes is being accurately described by the ECP/VBS scheme.

Shown in **1** is a model of Schrock's Lewis acid-free olefin metathesis catalysis [15]. The results for these catalyst models make good illustrative examples since they contain single, double and triple bonds from the transition metal M to the main group atoms (O, N, C) that have a variety of polarities [14b]. At the time of this study, experimental structures were available for M ≡ Mo, W; X ≡ N. Subsequently, the M ≡ Re; X ≡ C analog was published by Toreki et al. [15b]. Comparison of the experimental and calculated data in Table 1 shows that predicted bond lengths and bond angles involving the central metal deviate from the experimental system by an average of 0.01 Å and 2° respectively.

The ability of related TM complexes to occur in a wide variety of chemical environments is a hallmark of their chemistry, and one which must be handled by any computational scheme. Recent studies of Re–oxo compounds [14n] (**2**–**5**) provide a good illustration of the flexibility of the SBJK ECP scheme. The ECP

Table 1
Schrock's Lewis acid-free olefin metathesis catalyst models[a]

Bond length/angle	Mo (calc.)	Mo (expt.)	W (calc.)	W (expt.)	Re (calc.)	Re (expt.)
M=C (Å)	1.88	1.88	1.89	1.87	1.88	1.88
M≡X (Å)	1.71	1.73	1.72	1.73	1.70	1.70
M–O (Å)	1.90	1.87	1.90	1.88	1.91	1.92
O–M–O (°)	108	107	107	110	113	120
O–M=C (°)	107	109	108	110	110	107
C=M≡X (°)	102	100	103	103	97	96
O–M≡X (°)	116	115	115	112	112	112

[a] Experimental data are given in Ref. [15] (see **1**).

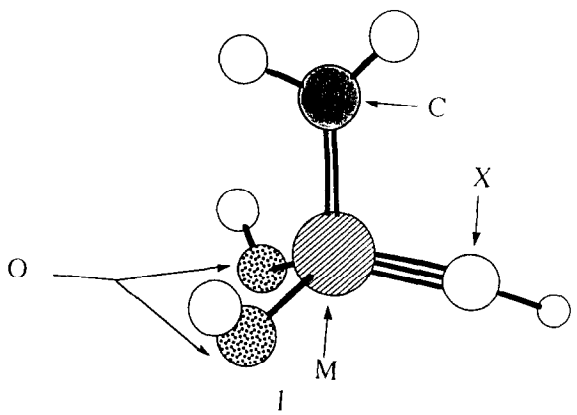

1

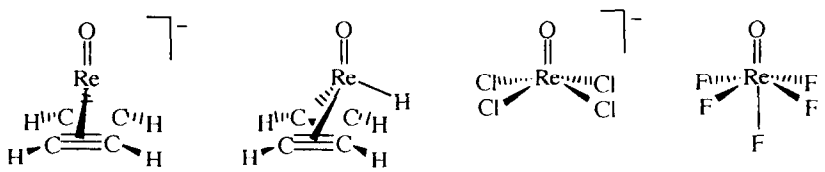

2 **3** **4** **5**

calculated structures (Table 2) show good agreement with experimental values, as determined by X-ray crystallography, for Re–oxo complexes with formal oxidation states of +7, +5, +3 and +1, and coordination numbers (counting acetylene as occupying one coordination site) of 3, 4, 5 and 6. Average deviations between calculated structures and experimental models is 0.03 Å and 2°. In the case of the bis(acetylene) Re–oxo anion **2**, the ECP calculations are able to reproduce subtle geometric perturbations, such as pivoting of the olefins, slight movement of the Re out of the plane defined by the oxo and the C≡C centers and splaying of the acetylenes such that the C≡C vectors are not parallel [14n]. The ECP results were

Table 2
Comparison of calculated and experimental Re–oxo geometries[a]

Bond length/angle	ReF_5O		Bond length/angle	$[ReCl_4O^-]$	
	Calc.	Expt.		Calc.	Expt.
Re–O (Å)	1.63	1.64	Re–O (Å)	1.62	1.63
$Re-F_{cis}$ (Å)	1.82	1.81	Re–Cl (Å)	2.39	2.34
$Re-F_{trans}$ (Å)	1.88	NR[b]	O–Re–Cl (°)	106	100
$O-Re-F_{cis}$ (°)	95	93			
Bond length/angle	$Re(O)(H)(C_2H_2)_2$[c]		Bond length/angle	$[Re(O)(C_2H_2)_2]^-$[c]	
	Calc.	Expt.		Calc.	Expt.
Re–O (Å)	1.66	1.70	Re–O (Å)	1.71	1.75
$Re-C_A$ (Å)	2.06	2.06	$Re-C_A$ (Å)	2.04	1.99
$Re-C_B$ (Å)	2.06	2.04	$Re-C_B$ (Å)	2.05	2.02
C_A-C_B (Å)	1.30	1.28	C_A-C_B (Å)	1.33	1.29
$O-Re-C_A$ (Å)	115	115	$O-Re-C_A$ (°)	124	124
$O-Re-C_B$ (°)	114	109	$O-Re-C_B$ (°)	114	114
Re–H (Å)	1.66	1.68[d]			
O–Re–H (°)	109	109[e]			

[a] Calculated geometries were determined at the RHF level using ECPs and valence basis sets described in Section 3. The calculated minima for ReF_5O and $ReCl_4O^-$ are C_{4v}; the calculated minima for the bis(acetylene) complexes are C_s.
[b] NR, not reported.
[c] The atoms denoted C_A and C_B represent the symmetry equivalent pairs in the C_s minima which are proximal and distal respectively with respect to the hydride ligand (iodide in the experimental model) and "open" end in the anion.
[d] The Re–H distance is that reported for $[ReH_9]^{2-}$ [16].
[e] The experimental value is the O–Re–I angle in $Re(O)(I)(C_2Me_2)_2$.

important in assessing whether the perturbations in the crystal structure of the Na(cryptand)$^+$ salt were due to the cation or crystal packing forces [14n].

Despite the flexibility built into the VBS, one concern which needs to be kept in mind when dealing with d block metals is the importance of electron correlation. A good example is provided by $Mn(=NMe)_3(Cl)$ in C_3 symmetry, a model of the interesting Mn^{VII}–tris(imido) complex ($Mn(=NCMe_3)_3(Cl)$) recently characterized by Wilkinson et al. [17]. Although the complex is d^0 (which tends to mitigate the electron correlation problem to a great extent), it is apparent that a flexible VBS is not sufficient to describe the electronic structure of this Mn–tris(imido) complex; deviation of the calculated C_3 structure for $Mn(=NMe)_3Cl$ (**6**) from the approximately C_3 $Mn(=NCMe_3)_3$ experimental structure (given in parentheses) is very large. Based on our studies of TM multiple bonding, it is found that, for a given family of compounds (e.g. imidos), the importance of electron correlation for an accurate description of ground state properties increases as one goes from the right to the left in a transition series and from heavier to lighter members of a triad,

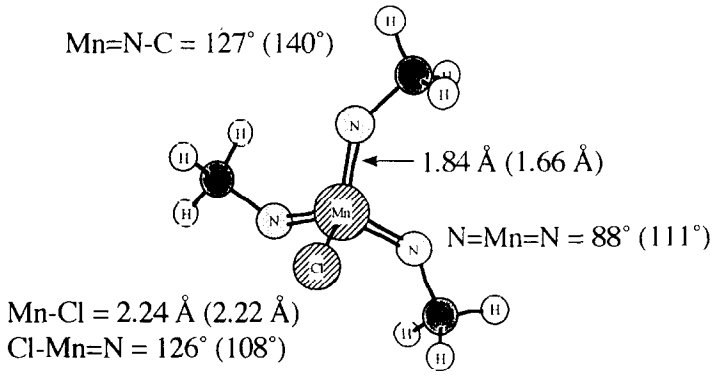

6

even for coordinatively saturated complexes [9,14]. Hartree–Fock optimization of a related tris(imido) for the element following Mn in Group VIIB, i.e. $(HN=)_3Tc-Tc(=NH)_3$, shows excellent agreement with the structure of ethane-like $Tc_2(=NAr)_6$ (Ar, 2,6-diisopropyl-phenyl) reported by Bryan and Burrell [18]: Tc—Tc = 2.72 Å (2.744(1) Å, expt.); Tc=N = 1.73 Å (1.758(2) Å, expt.); N=Tc—Tc = 100° (103.6(1)°, expt.); N=Tc=N = 117° (114.6(1)°, expt.). It seems likely that an accurate treatment of **6** will entail extensive correlation with multiconfiguration wavefunctions, although tests with more extensive basis sets than used in the standard SBKJ scheme (at Hartree–Fock and correlated levels) would be advisable. As noted above, a key ingredient in the calculations that facilitates extensive study of larger (and typically more experimentally relevant) TM species is the availability of a version of an electronic structure code for parallel computers. Development of such codes for correlated wavefunctions, such as used in the MCSCF, CI or MP2 levels of theory, is a much greater challenge than for SCF wavefunctions. A parallel algorithm for calculating MCSCF wavefunctions has very recently been developed for GAMESS [19]. These advances in parallel computing will afford the opportunity to study such interesting species as **6**.

4.2. Multiple bonding involving heavier MG elements

Recently there has been greater effort directed towards the synthesis of complexes with multiple bonds between TMs and heavier MG elements [13]. Apart from the fundamental interest in multiple bonding involving heavier MG elements, such complexes have been envisioned as precursors for materials such as TM sulfides, phosphides and silicides [13]. Multiple bonds involving these elements can present greater computational challenges in relation to lighter congeners since an explicit account of electron correlation may be needed as the MG element becomes heavier and TM—MG π bonding becomes weaker. Studies of high-valent silylidene complexes ($L_nM=Si(R)R'$) showed that while the M—Si σ bond could be described with a Hartree–Fock wavefunction, the M—Si π bond needed a multideterminant

description to allow for mixing in states such as $(\pi_{MSi})^0(\pi_{MSi}^*)^2$ into the dominant $(\pi_{MSi})^2(\pi_{MSi}^*)^0$ configuration [14d,e].

There is a growing body of data for one family of TM=MG (heavy) complexes, the chalcogenides. An excellent series of complexes is provided by Parkin and Howard [13e], who have reported $Cp'_2M(E)py$ (**7a**). Through parallel supercomputing and ECP methods, we were able to study the structures of the parent Cp_2ME compounds (**7b**). The calculated ME bond lengths at the RHF level are ZrO = 1.76 Å (1.804(4) Å), ZrS = 2.28 Å (2.334(2) Å), ZrSe = 2.42 Å (2.480(1) Å) and ZrTe = 2.68 Å (2.729(1) Å) [13e]. Similar good agreement is found for Hf analogs [14o]. The Ti–oxo bond length in Cp_2TiO is 1.61 Å [14o], in acceptable agreement with $Cp^*_2Ti(O)$(4-phenyl-py) ($Cp^* \equiv \eta^5$-C_5Me_5) which has TiO = 1.665(3) Å [20]. The results for Group IVB chalcogenides should be contrasted with those for TM=Si complexes [14d,e], where a multiconfigurational wavefunction constitutes a minimum acceptable level of theory, and further emphasize the necessity for calibration of computational results against extant experimental data in the study of a new family of complexes. Uniformly good agreement [14o] between theory and experiment from the lightest (Cp_2TiO) to the heaviest (Cp_2HfTe) member in the series is a clear demonstration of the power of ECP methods as a tool in opening up all areas of the Periodic Table to computation.

4.3. Electronic structure

TM multiple bonding provides much fertile ground for research, since it is the key to understanding their behavior in many important reactions [12]. Explanations of the experimentally observed chemistry of TM=MG complexes are often couched in valence bond terms, i.e. which resonance (or Lewis) structure dominates in a given situation. For example, the metal–carbon linkage in alkylidenes has been described

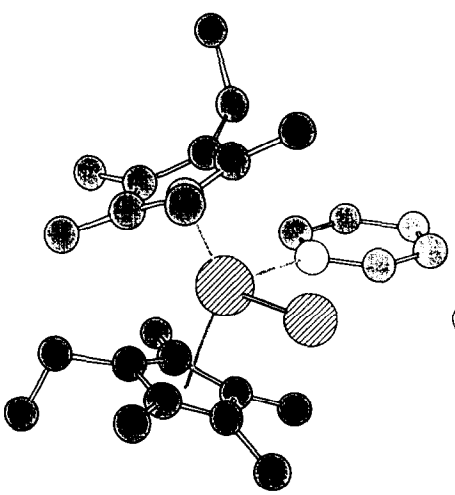

7a

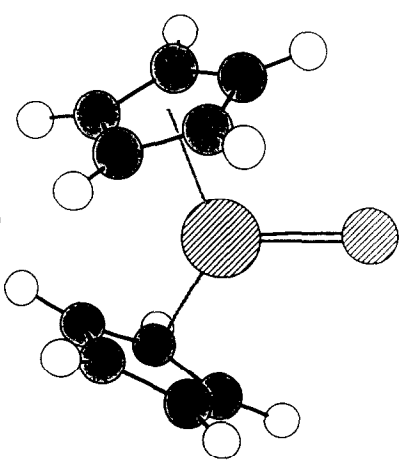

7b

as ethylene-like (**A**), a π-ylide (**B**), coordinated singlet carbene (**C**) or a four-electron donor (**D**), as shown in Eq. (2) [21].

$$\underset{\mathbf{A}}{M{=}C} \quad \underset{\mathbf{B}}{M{\leftleftharpoons}C} \quad \underset{\mathbf{C}}{M{\rightleftharpoons}C} \quad \underset{\mathbf{D}}{M{\leftharpoonup}C} \tag{2}$$

Similar resonance structure descriptions for imido and oxo complexes can also be found in the literature [12]. Typically these descriptions are based on the observed reactivity. For example, the ability of high-valent alkylidenes to olefinate carbonyls in the manner of phosphorus-based Wittig reagents suggests a π-ylide description of the metal–alkylidene bond (**B**) [21c]. Resonance structure descriptions have also been inferred from structural data. For example, a linear coordination mode for imido complexes is suggestive of a triple bond description (**E**), while bent imidos are envisioned as being coordinated through a metal–nitrogen double bond (**F**) [12,22].

The utility of chemically intuitive Lewis structure descriptions such as **A–F** is clear, since such structures are easily related to simple valance bond-like concepts and can be used to understand and rationalize TM=MG bonding and reactivity. The MCSCF/LMO/CI scheme outlined earlier can be thought of as a bridge between complicated and highly accurate ab initio molecular orbital-based calculations and the appealing visual picture provided by Lewis structures. The technique is easily used to provide a Lewis structure-like description of any multiple bond. The localization process serves to transform the MOs into those necessary to describe the bond of interest. The AO-like MOs are highly localized on either end of the multiple bond, although they possess small "tails" (typically less than 2%) on the atom comprising the other end of the bond. The presence of these small tails is necessary to ensure orthogonality among the final orbitals, and this distinguishes the MCSCF/LMO/CI method from the spin-coupled valence bond approach [23]. The small tails in the localized orbitals make the computational problem much more tractable and therefore the MCSCF/LMO/CI method is applicable to larger TM complexes. It is critical to recognize that the MCSCF/LMO/CI technique provides an alternative (and chemically appealing) conceptual picture of the basic nature of bonding in the compound of interest. The procedure does not alter the total molecular wavefunction (and therefore the fundamental quantum mechanical description of the TM=MG complex) at all. We are, in a sense, taking a photograph of the same object with a different lens.

For double (triple) bonds, there are 20 (175) resonance structures that can be obtained from the distribution of four (six) electrons in four (six) AO-like MOs, with the constraint that there be equal numbers of up- and down-spin electrons. While this seems to be a large number of configurations (resonance structures) to deal with, analysis of the bond of interest is simplified by the fact that not all descriptions of

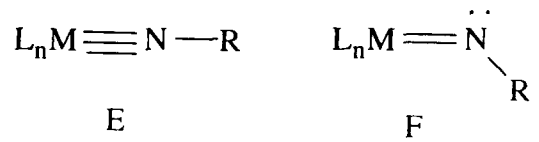

E F

a bond are chemically reasonable. For example, while **G** is certainly plausible (i.e. a pair of two-electron bonds), the presence of a three-electron σ bond and one-electron π bond in structure **H** suggests that its importance in describing the linkage will be minimal. If one considers as chemically reasonable only those resonance structures that have two-center, two-electron bonds, then the number of resonance structures to be examined drops dramatically. It is gratifying that the outcome of the MCSCF/LMO/CI procedure is that only those resonance structures which are chemically sensible by this definition have significant weights in the final wavefunction. This will be illustrated quantitatively below. The nine chemically sensible resonance structures for a double bond are shown in Eq. (3).

$$\begin{array}{lll} M=E & M\leftarrow E & M\rightarrow E \\ M\rightleftharpoons E & M\leftrightarrows E & M\rightrightarrows E \\ M\leftleftharpoons E & M\leftleftarrows E & M\leftrightarrows E \end{array} \qquad (3)$$

A straight line represents a covalent bond (i.e. one electron in a TM-centered AO-like MO and one in the MG-centered counterpart), an arrow pointing towards the metal represents a dative bond (both electrons on the MG-centered AO-like MO) and an arrow pointing towards the element is described as a back bond (i.e. both electrons on the TM-centered AO-like MO). The bottom line (or arrow) describes the σ bond and the other lines the π components of the ME linkage. The 27 "chemical" resonance structures which describe a triple bond can be found elsewhere [14f].

To facilitate discussion of the resonance structure, it is also possible to subdivide them further into nucleophilic, electrophilic and neutral contibutions. Nucleophilic and electrophilic resonance structures are defined as those in which the formal charge on the MG element is negative and positive respectively. Any bonds the MG element makes to substituents are considered to be covalent, contributing one electron to the MG element for each MG–substituent bond. Thus resonance structures **A** and **C** in Eq. (2) are neutral, while **B** and **D** are nucleophilic.

It is satisfying that the MCSCF/LMO/CI technique reveals that the so-called "chemical" resonance structures dominate [14]. For all multiply bonded species investigated to date, the chemically sensible resonance structures make the overwhelming contribution (95% or more) to the total wavefunction. It is expected that

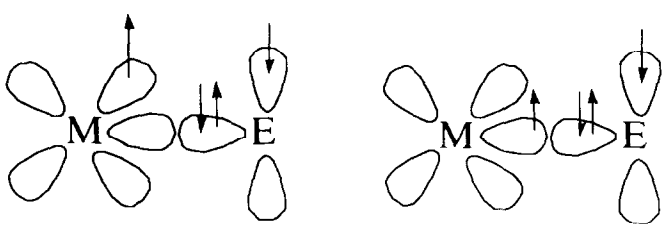

G H

M⇌E **M⇄E**

the resonance structures in which the MG element acts as a σ donor will be much more important than those where it acts as a σ acceptor. Similarly, it is expected that back-bonding resonance structures will be more prevalent in the π bond(s). Finally, for the coordination of MG fragments to early, high-valent TMs, resonance structures which are nucleophilic and neutral should dominate over electrophilic resonance structures. As one goes to lower valent complexes, this trend is expected to start to reverse. Each of these chemically intuitive expectations is supported by the MCSCF/LMO/CI analysis. This not only provides confidence in the MCSCF/LMO/CI method, but also in the underlying ECP/VBS description [14] of the TM=MG complex on which it is based.

To illustrate the power of MCSCF/LMO/CI, we present results for both double and triple bonds. The doubly bonded species will provide a comparison between alkylidene and silylidene complexes, while the focus will be on imido complexes for the description of triple bonds.

An important consideration in describing an M=E bond is that an appropriate level of theory is used to describe the wavefunction. In particular, it is important to be aware of the amount of configurational mixing present in the correct wavefunction. As noted earlier, in the limit that a closed shell (RHF) description is valid, there will be no configurational mixing. An equivalent way of saying this is that the wavefunction has no "diradical character", i.e. the natural orbital occupation numbers (NOONs) of the bonding MOs (e.g. σ and π) will be identically 2.0, while the NOONs of the antibonding MOs (e.g. σ* and π*) will be 0.0. As the diradical character increases, the bonding NOONs decrease to values of less than 2.0, while the antibonding NOONs increase to values greater than 0.0. A "pure" π diradical would have NOON(π) = NOON(π*) = 1.0. For all M=E bonds investigated to date, the amount of configurational mixing in the σ framework has been very small, so NOON(σ) ≈ 2.0 and NOON(σ*) ≈ 0.0. The same is not true for the π bonds, however. Here, there can be considerable configurational mixing, and therefore considerable diradical character. As an example, let us consider a series of M=Si bonds in which both the transition metal M and the substituents at both the TM and Si ends are varied. The results are summarized in Table 3, where n is the NOON and k_{MSi} is the MSi force constant (mdyn $Å^{-1}$). First, let us consider the effect of varying M. Within Group IVB, the diradical character, as measured by the NOON, clearly decreases as the TM gets heavier (Ti > Zr > Hf). Since diradical character implies kinetic instability (high reactivity), this is also the order of increasing kinetic stability (i.e. Hf > Zr > Ti). Interestingly, the force constant for the MSi bond increases in the same direction, so thermodynamic stability increases in the same order. This should not imply very strong π bonds, however, since all force constants in Table 3 are still smaller than those for very weak Sn=Sn and Sn=Ge bonds [24]. The same trends are observed in Group VB, since the diradical character in the Ta=Si bond is generally smaller than that in the corresponding Nb=Si bond, and the force constant is correspondingly larger. Finally, both the kinetic and thermodynamic stabilities are greater for a Group VB element than for the Group IVB element in the same row. It is clear that an MCSCF wavefunction that at least correlates the

Table 3
Metal–silicon force constants and π populations[a]

	$H_2M{=}SiH_2$	$Cl_2M{=}SiH_2$	$H_2M{=}SiHCl$	$H_2M{=}SiCl_2$	$H_2M{=}SiHMe$	$H_2M{=}Si(H)SiH_3$
M ≡ Ti						
k_{MSi}	1.30	1.57	1.36	1.41	1.37	1.26
n_π	1.557	1.653	1.594	1.637	1.598	1.533
n_{π^*}	0.443	0.347	0.406	0.363	0.402	0.467
M ≡ Zr						
k_{MSi}	1.49	1.59	1.38	1.40	1.40	1.50
n_π	1.748	1.783	1.765	1.788	1.771	1.737
n_{π^*}	0.252	0.217	0.235	0.212	0.229	0.263
M ≡ Hf						
k_{MSi}	1.56	1.78	1.60	1.63	1.60	1.52
n_π	1.805	1.821	1.817	1.823	1.821	1.801
n_{π^*}	0.195	0.179	0.183	0.168	0.179	0.199
M ≡ Nb						
k_{MSi}	1.77	1.92	1.80	1.71	1.83	1.73
n_π	1.769	1.792	1.804	1.824	1.804	1.757
n_{π^*}	0.231	0.208	0.196	0.176	0.196	0.243
M ≡ Ta						
k_{MSi}	1.86	2.03	1.90	1.86	1.95	1.99
n_π	1.805	1.804	1.825	1.838	1.829	1.795
n_{π^*}	0.195	0.196	0.175	0.162	0.171	0.205

[a] Equilibrium force constants (k_{MSi}, mdyn $Å^{-1}$) and π bonding (n_π) and π antibonding (n_{π^*}) MO occupations are calculated at the two-configuration self-consistent field (TCSCF) level of theory using the basis sets described in the text and in Ref. [14e].

π space is necessary for all of these compounds, since the number of electrons in the π* orbital is substantial (greater than 0.16) for all of the M=Si compounds.

Replacing the hydrogens on M with chlorines generally decreases the diradical character in the M=Si bond (although Ta is an exception) and also tends to increase the MSi force constant (Table 3). Making the analogous substitution at the Si end has the same effect on the diradical character, but not necessarily on the force constant. Methyl substitution at the Si end has an effect similar to that of Cl, while silyl substitution at the Si end has a small impact on the bond stability. Therefore the most stable M=Si bonds, from both a thermodynamic and kinetic point of view, are those between Si and Ta, especially with Cl substituents. To the extent that Cl is a reasonable prototype for Cp in these complexes [14e], calculations suggest three synthetic strategies for Cp-substituted TM=Si complexes: (1) metals from the third transition series; (2) electron-withdrawing ligands; (3) Si substituents which are good π donors.

Contributions of the primary resonance structures to Group IVB and Group VB M=Si and M=C bonds are summarized in Table 4. For both C and Si, the two most important contributions to the total wavefunction are the covalent and the

Table 4
Resonance structure contributors for alkylidenes vs. silylidenes[a]

Resonance contributor	M ≡ Ti											
	$H_2M{=}EH_2$		$Cl_2M{=}EH_2$		$H_2M{=}EHCl$		$H_2Si{=}ECl_2$		$H_2M{=}SiHMe$		$H_2M{=}EHSiH_3$	
	Si	C	Si	C	Si	C	Si	C	Si	C	Si	C
M⇇E	0.3	2.6	0.3	1.6	0.3	2.1	0.2	1.9	0.3	2.3	0.3	3.5
M⇐E	1.9	9.7	2.3	7.1	1.7	7.2	1.4	5.6	2.0	9.3	2.0	13.5
M⇆E	0.8	2.3	1.0	2.0	0.8	1.7	0.7	1.3	0.9	2.3	0.9	3.0
M⇇E	34.6	36.2	30.3	33.8	33.3	39.1	31.4	42.0	34.1	34.1	35.2	35.0
M = E	44.6	36.5	42.7	40.0	43.7	36.4	42.9	35.8	43.1	37.6	45.3	33.9
M⇉E	5.4	2.6	4.3	3.2	6.0	2.6	6.7	2.6	4.9	2.8	5.2	2.3
M⇄E	8.2	7.3	13.2	8.9	9.2	8.0	10.2	8.0	10.0	8.3	7.5	6.5
M⇉E	3.8	2.6	5.4	3.4	4.6	2.7	5.7	2.6	4.4	3.1	3.3	2.1
M⇉E	0.2	0.1	0.3	0.1	0.3	0.1	0.5	0.1	0.3	0.1	0.2	0.1
Electrophilic	9.4	5.3	10.0	6.7	10.9	5.4	12.9	5.3	9.6	6.0	8.7	4.4
Nucleophilic	36.8	48.5	32.9	42.5	35.3	48.4	33.8	49.5	36.4	45.7	37.5	52.0
Neutral	53.6	46.1	56.9	50.9	53.7	46.1	53.8	45.1	54.0	48.2	53.7	43.4
Resonance contributor	M ≡ Zr											
	$H_2M{=}EH_2$		$Cl_2M{=}EH_2$		$H_2M{=}EHCl$		$H_2Si{=}ECl_2$		$H_2M{=}SiHMe$		$H_2M{=}EHSiH_3$	
	Si	C	Si	C	Si	C	Si	C	Si	C	Si	C
M⇇E	1.6	6.3	1.3	5.0	1.5	6.3	1.4	6.4	1.6	5.5	1.4	7.9
M⇐E	5.5	14.1	4.9	12.3	5.0	12.9	4.4	11.8	5.4	13.5	4.4	16.8
M⇆E	2.0	3.1	1.8	3.1	1.9	2.8	1.8	2.5	1.9	3.2	1.8	3.5
M⇇E	31.5	30.9	28.8	29.8	30.4	32.9	28.8	35.0	30.6	27.9	28.8	30.5
M = E	40.0	32.8	39.5	34.8	39.6	32.4	39.3	31.7	39.1	34.0	39.3	30.5
M⇉E	5.7	3.1	5.5	3.6	6.2	3.0	6.7	2.8	5.5	3.3	6.7	2.6
M⇄E	8.6	6.8	11.3	7.6	9.3	6.8	10.2	6.9	9.9	7.5	10.2	5.8
M⇉E	4.7	2.9	6.2	3.6	5.4	2.8	6.5	2.7	5.4	3.5	6.5	2.2
M⇉E	0.4	0.1	0.4	0.2	0.5	0.1	0.6	0.1	0.4	0.1	0.6	0.1
Electrophilic	10.8	6.1	12.1	7.4	12.1	5.7	13.8	5.6	1.3	6.9	13.8	4.9
Nucleophilic	38.6	51.4	35.0	47.1	36.9	52.0	34.6	53.2	37.6	46.9	34.6	55.2
Neutral	50.6	42.7	52.6	45.5	50.5	42.0	51.3	41.1	50.9	44.7	51.3	39.8
Resonance contributor	M ≡ Hf											
	$H_2M{=}EH_2$		$Cl_2M{=}EH_2$		$H_2M{=}EHCl$		$H_2Si{=}ECl_2$		$H_2M{=}SiHMe$		$H_2M{=}EHSiH_3$	
	Si	C	Si	C	Si	C	Si	C	Si	C	Si	C
M⇇E	2.4	8.1	2.0	6.8	2.2	8.2	1.9	8.4	2.3	7.3	2.5	10.0
M⇐E	7.7	15.1	7.0	13.6	7.1	14.3	6.4	13.5	7.5	14.7	8.4	17.4
M⇆E	3.1	3.1	2.7	3.0	3.0	2.9	2.9	2.7	2.9	3.2	3.3	3.3
M⇇E	27.8	31.1	26.8	30.6	26.6	32.7	25.2	34.2	27.2	29.7	27.8	30.8
M = E	39.4	30.4	39.3	32.2	39.5	30.1	39.4	29.4	39.0	31.7	39.4	28.2
M⇉E	6.7	2.8	6.6	3.2	7.5	2.8	8.1	2.7	6.8	3.1	6.8	2.4
M⇄E	7.3	6.4	9.0	7.1	7.8	6.4	8.4	6.4	8.2	7.0	6.8	5.6
M⇉E	4.9	2.7	5.9	3.2	5.6	2.6	6.5	2.5	5.5	3.2	4.5	2.2
M⇉E	0.5	0.1	0.5	0.1	0.6	0.1	0.8	0.1	0.5	0.1	0.4	0.1
Electrophilic	12.1	5.6	13.0	6.6	13.7	5.6	15.4	5.3	12.8	6.4	11.7	4.7
Nucleophilic	37.9	54.3	35.8	51.0	35.9	55.2	33.5	56.1	37.0	51.7	38.9	58.2
Neutral	50.2	40.3	51.0	42.3	50.3	39.4	50.7	38.5	50.1	41.9	49.5	37.1

Table 4 (continued)

Resonance contributor	M ≡ Nb											
	$H_2M{=}EH_2$		$Cl_2M{=}EH_2$		$H_2M{=}EHCl$		$H_2Si{=}ECl_2$		$H_2M{=}SiHMe$		$H_2M{=}EHSiH_3$	
	Si	C	Si	C	Si	C	Si	C	Si	C	Si	C
M⇇E	0.9	3.7	0.5	2.6	0.9	3.3	0.8	3.5	0.9	3.1	0.9	4.6
M⇐E	4.8	11.7	3.6	9.7	4.2	10.2	3.5	9.4	4.5	11.0	5.3	14.2
M⇆E	1.9	3.5	1.8	3.4	1.6	2.9	1.3	2.5	1.7	3.4	2.1	4.0
M⇐E	24.1	26.3	19.3	24.0	25.8	27.4	26.0	30.6	24.4	24.6	25.3	25.8
M=E	41.5	37.4	43.4	40.1	39.0	37.9	36.9	36.3	40.1	38.5	42.5	36.0
M⇒E	5.3	4.4	6.8	5.5	4.9	4.3	4.8	3.8	5.0	4.8	5.2	4.1
M⇄E	13.2	8.1	13.7	8.8	15.1	8.8	16.8	9.2	14.6	8.9	11.6	7.0
M⇒E	7.6	4.5	9.9	5.6	7.9	4.9	8.8	4.4	8.1	5.4	6.5	3.8
M⇉E	0.5	0.2	0.7	0.3	0.5	0.2	0.6	0.2	0.5	0.3	0.4	0.2
Electrophilic	13.4	9.1	17.4	11.4	13.3	9.4	14.2	8.4	13.6	10.5	12.1	8.0
Nucleophilic	29.8	41.7	23.4	36.3	30.9	40.9	30.3	43.5	29.9	38.7	31.5	44.6
Neutral	56.0	49.0	58.9	52.3	55.7	49.6	55.0	48.0	56.4	50.8	56.2	47.0
Resonance contributor	M ≡ Ta											
	$H_2M{=}EH_2$		$Cl_2M{=}EH_2$		$H_2M{=}EHCl$		$H_2Si{=}ECl_2$		$H_2M{=}SiHMe$		$H_2M{=}EHSiH_3$	
	Si	C	Si	C	Si	C	Si	C	Si	C	Si	C
M⇇E	1.5	5.5	1.0	4.3	1.4	5.2	1.3	5.3	1.5	4.8	1.6	6.8
M⇐E	6.3	13.4	5.2	11.9	5.6	12.0	4.8	11.3	6.1	12.8	7.0	15.8
M⇆E	2.3	3.3	2.2	3.3	2.1	2.9	1.9	2.6	2.2	3.3	2.6	3.7
M⇐E	26.5	28.2	22.5	26.7	26.1	29.8	25.7	31.7	25.5	26.6	26.4	27.8
M=E	39.7	34.1	41.7	36.1	38.8	33.9	37.9	33.3	39.0	35.1	40.3	32.4
M⇒E	5.5	3.7	6.7	4.5	5.7	3.6	5.9	3.4	5.4	4.0	5.5	3.3
M⇄E	11.0	7.6	11.6	8.1	12.1	8.1	13.1	8.3	12.3	8.3	10.0	6.8
M⇒E	6.5	3.9	8.3	4.6	7.4	4.0	8.3	3.8	7.5	4.7	6.0	3.3
M⇉E	0.5	0.2	0.7	0.3	0.6	0.2	0.7	0.2	0.5	0.2	0.4	0.2
Electrophilic	12.5	7.8	15.7	9.4	13.7	7.8	14.9	7.4	13.4	8.9	11.9	6.7
Nucleophilic	35.3	47.1	28.2	42.9	33.0	47.0	31.8	48.3	33.1	44.2	35.0	50.4
Neutral	53.0	45.0	55.5	47.5	53.0	44.9	52.9	44.2	53.5	46.7	52.9	42.9

[a] Contributions from nine "chemical" resonance structures for the TM–MG multiple bond in analogous alkylidenes ($L_nM{=}C(R)R'$) and silylidenes ($L_nM{=}Si(R)R'$) (see text for further descriptions of resonance classifications).

σ dative/π covalent structure (σ-ylide)

M=E M⇐E

These two structures account for 60%–80% of the total wavefunction for both E ≡ C and E ≡ Si. The σ-ylide does not correspond to a resonance structure discussed previously in the literature and thus highlights the use of MCSCF/LMO/CI to not only confirm, but augment, our understanding of bonding as deduced from the observed structure and reactivity. The remainder of the wavefunction is distributed among the other seven "chemical" structures shown in Eq. (3). There is only a modest variation as a function of the metal or substituent. The breakdown among

neutral, nucleophilic and electrophilic contributions, also summarised in Table 4, provides an interesting contrast between Si and C. As discussed above, we generally expect the electrophilic contribution to be smaller than the other two, and this is found to be the case. However, the electrophilic contribution is generally much larger when E ≡ Si than when E ≡ C. This reflects the greater electronegativity of C vs. Si. Consistent with this, neutral resonance structures are much more important in M=Si wavefunctions than in M=C wavefunctions. In the latter, the neutral and nucleophilic resonance structures have roughly equal weights.

Let us consider the application of MCSCF/LMO/CI to imido complexes. There are eight resonance structures (Fig. 2) to be considered for a ground state description of TM–imidos. We treat both π components as equal in Fig. 2; although not rigorously correct, π bonds perpendicular and parallel to the MNX plane display similar behavior for large M=N−X angles [14f].

The eight structures in Fig. 2 account for over 90% of the total contributions to the ground state description of the metal–imido linkage. Six resonance structures correspond to descriptions found in the literature. Perhaps the most important point to emerge from the MCSCF/LMO/CI analysis is that the TM=MG multiple bond cannot be described as being dominated by a single resonance structure. Modification of a TM=MG complex for synthetic or catalytic advantage will not cause one resonance structure to dominate, but will affect the subtle interplay of dominant resonance structures. For example, MCSCF/LMO/CI results for silylidene [14e] (L_nM=Si(R)R′) and alkylidene [14a] complexes show the π donor character of Cl to be more important than the effect on the σ framework brought about by its electronegativity. The MCSCF/LMO/CI analysis shows in a quantitative manner which resonance contributors are changing and thus how the TM, ligand and/or substituent affects the TM=MG bond.

In Fig. 3, the changes in resonance contributors are shown as a function of

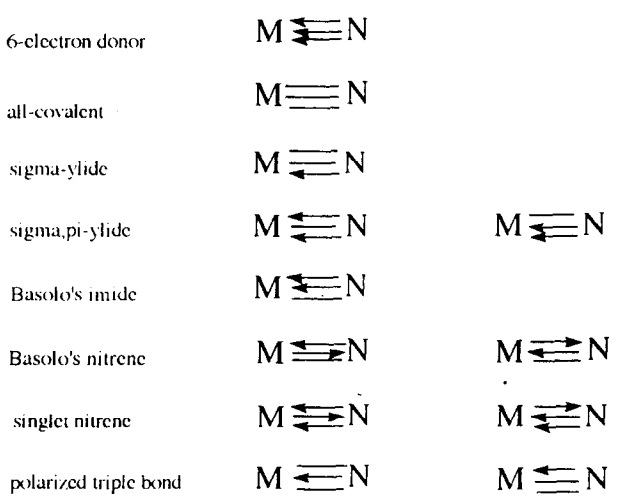

Fig. 2. Eight principal resonance contributors to the TM–imido bond.

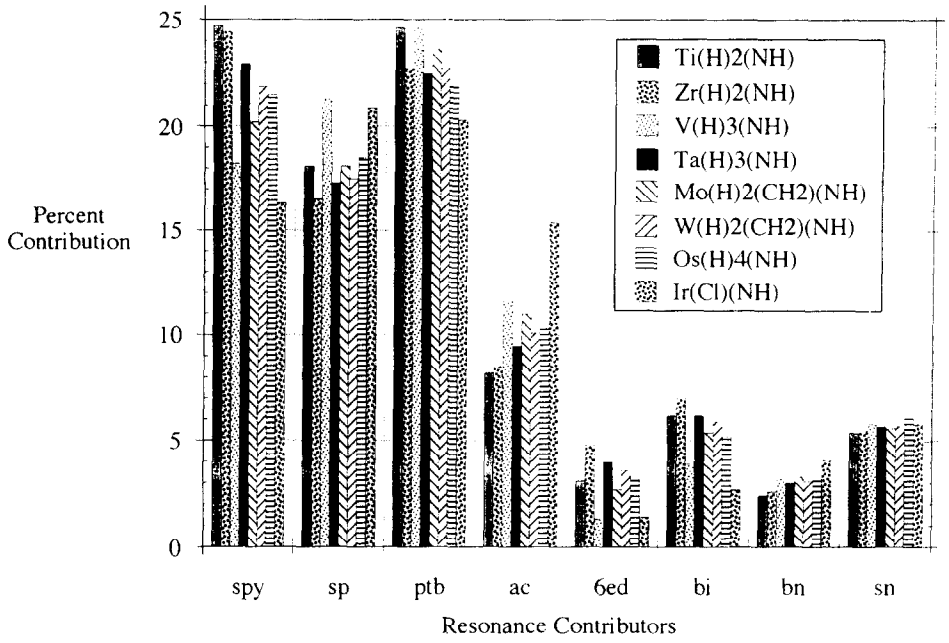

Fig. 3. Changes in eight prime resonance contributors as a function of the metal.

changing the central TM. Complexes with experimental models are chosen [12d]. The singlet nitrene (sn) (Fig. 2) changes the least in Fig. 3. For the two neutral structures, σ-ylide (sy) and polarized triple bond (ptb), a different behavior is exhibited. The σ-ylide, with its dative σ bond, increases in importance from left to right in the transition series, while the ptb structure decreases from left to right. The nucleophilic structures — σ,π-ylide (spy), Basolo's imide (bi) and the six-electron donor (6ed) — are largest for the early metals and generally decrease as one proceeds to the left, particularly for the σ,π-ylide (see Fig. 3). The electrophilic structures — the all-covalent (ac) and Basolo's nitrene (bn) — show the opposite trend. Changes in the TM–imido bond concur with the concepts first suggested by Nugent et al. [25]. Thus MCSCF/LMO/CI clearly shows changes in contributions from the various resonance structures which are in accord with, and contribute to, changes in chemical reactivity.

4.4. Reactivity

An essential use of TMs and TM complexes is as catalysts for a broad range of chemical reactions, such as activation of bonds in alkanes, hydrosilation and a variety of polymerization reactions [1,12]. The importance of reactive intermediates and transition states in catalysis, species for which direct experimental evidence is often limited, makes catalysis an ideal area for computational studies. While we have an interest in many catalytically important processes, in the following we focus on

recent calculations of TM activation of methane by Co^+ and by a series of prototypical complexes.

Selective C—H activation is the first, and often most difficult, step in important processes such as catalytic methane conversion. The desire to effect direct, catalytic conversion of abundant methane to liquid fuels and more easily transportable materials (e.g. methanol) has attracted the efforts of many chemists [26]. Scission of C—H can be either a non-concerted or concerted process [27]. Non-concerted systems activate through homolytic (e.g. biochemical oxidation [28]) or heterolytic (e.g. superacid systems [29]) C—H cleavage. Non-concerted C—H activation tends to yield low selectivity; thus much interest has focused on concerted C—H activation [30–43]. The two recognized concerted C—H activation mechanisms are [2 + 2] [30–33] and oxidative [34–42] addition. The [2 + 2] mechanism involves 1,2-addition of C—H across a metal–ligand single (σ bond metathesis [31,33]) or multiple ($[2_\sigma + 2_\pi]$ addition [32]) bond and is effected by high-valent (d^0 or d^0f^n) complexes [30]; examples include $Cp^*_2LuCH_3$ [31], $(NHSi')_2Zr{=}NSi'$ ($Si' \equiv Si(t\text{-}Bu)_3$) [32a] and thoracyclobutanes [33]. Oxidative addition entails 1,1-addition of C—H to a low-valent TM and increases the formal oxidation state and coordination number of the TM by two units [34,35]. Sixteen-electron $Cp^*M(L)$ ($M \equiv Rh$, Ir; $L \equiv PR_3$, CO) [36–38] and fourteen-electron $M(L)_n(PR_3)_m$ ($L \equiv$ univalent ligand such as hydrido, chloro or an η^1-carboxylate and $M \equiv Ir$, Rh) [39–42] species are known for which oxidative addition is the putative C—H activation mechanism.

Reactions between atomic TM ions and alkanes in the gas phase yield much insight into the kinetics and thermodynamics [43] of similar processes in condensed phases. The potential energy surfaces (PESs) for the reaction of Co^+ (^3F, s^1d^7) with methane and the reverse reaction of $CoCH_2^+$ (in several of its low-lying electronic states) with H_2 have been studied using ECP basis sets and MRCI wavefunctions [44]. The reactions are qualitatively similar for all $CoCH_2^+$ electronic states, since they differ primarily in the identity of the occupied non-bonding Co^+ d orbitals. A typical potential energy curve is illustrated in Fig. 4 for the lowest $^3A'$ (broken curve) and $^3A''$ (full curve) states. There are several stationary points (minima and transition states) of interest on these curves. On the far right of the figure are the separated species $Co^+ + CH_4$. As these species approach each other, they form a complex $[Co \cdots CH_4]^+$. The structure of this complex may be either C_{2v} (with two of the four hydrogens bound to the metal, **8a**) or C_{3v} (in which three of the hydrogens are bound to the metal, **8b**). At the MRCI level, the Hay–Wadt ECP predicts that the two structures are virtually degenerate, whereas the SBKJ ECP finds the C_{2v} structure to be lower by about 6 kcal mol^{-1}. All calculations predict that a C_{3v} structure with just one H bound to the metal ($Co^+ — H — C = 180°$) is much higher in energy. The most recent experimental measurement [45] of the binding energy of Co^+ to methane is 22.9 ± 0.7 kcal mol^{-1}. The MRCI/SBKJ prediction of 22.3 kcal mol^{-1} is in very good agreement with the experimental value.

Proceeding to the left in Fig. 4 brings us to a transition state that separates the methane adduct from $HCoCH_3^+$. The MRCI/SBKJ barrier that separates $HCoCH_3^+$ from the final complex is very small (2.6 kcal mol^{-1}), so it is very possible that the

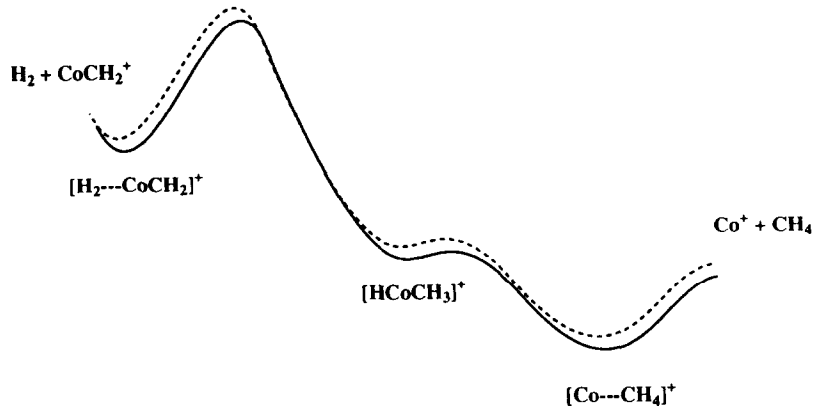

Fig. 4. Schematic potential energy surfaces for methane activation by Co^+. Full curve, A''; broken curve, A'.

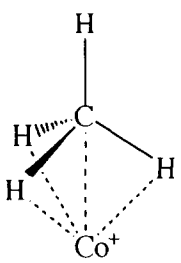

8a

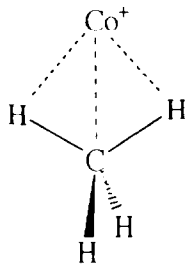

8b

$HCoCH_3^+$ species does not exist. Indeed, use of the HW ECP predicts that this barrier disappears when the multireference CI is added to the MCSCF wavefunction. The next step on the reaction surface is the transfer of a second hydrogen to the metal to form $(H_2)CoCH_2^+$, a complex between H_2 and $CoCH_2^+$. The barrier for this process is substantial (above 30 kcal mol^{-1}) in both the forward and reverse directions. So, at thermal energies, this barrier is expected to prohibit further progress in either direction. The complex between H_2 and $CoCH_2^+$ is predicted to be bound by about 8.5 kcal mol^{-1} at the MRCI/SBKJ level of theory. The binding energy of the species $CoCH_2$* itself is predicted to be 78–80 kcal mol^{-1}, in excellent agreement with the experimental values of 77.5 ± 2.3 kcal mol^{-1} (ion beam experiment [46]) and 84 ± 5 kcal mol^{-1} (gas phase photodissociation [47]).

Based on the PES in Fig. 4, the reaction of Co^+ with CH_4 may yield the ion–molecule complex as the only stable product. This is in agreement with available experimental data [48]. The species CoH^+ and $CoCH_3^+$ have also been studied at the same levels of theory [44]. While the reaction $Co^+ + CH_4 \rightarrow CoCH_2^+ + H_2$ is predicted to be slightly more favourable thermodynamically than the reactions $Co^+ + CH_4 \rightarrow CoCH_3^+ + H$ and $Co^+ + CH_4 \rightarrow CoH^+ + CH_3$, the high predicted barrier for the former may mean that the latter may be preferred at elevated temperatures.

The results for methane activation by Co^+ emphasize a paradox of computational TM chemistry, i.e. larger, coordinatively saturated species are often easier to treat than smaller, coordinatively unsaturated complexes. The presence of a ligand field limits the number of low-energy excited states, so that lower level (and computationally less intensive) methods are often appropriate for coordinatively saturated systems. Gas phase chemistry has provided a greater amount of thermodynamic data, once nearly non-existent, for TM species [43]. The use of chemically sensible theoretical approaches to study reactions such as $Co^+ + CH_4$ will not only yield insight into important chemistry, but provide further checks on the methods of evaluation of accurate thermodynamic and kinetic data for reactions involving TMs.

Systems which are intermediate between the extremes of late, low-valent complexes (which effect C—H activation through oxidative addition) and early, high-valent complexes (which effect C—H activation by [2 + 2] addition) have recently garnered attention as practical methane functionalization catalysts [49–54]. These systems possess late, but electrophilic, TMs and are stable at ambient temperatures and in the presence of O_2 and H_2O [54]. The C—H activation mechanism for these complexes is unclear. To build towards an understanding of electrophilic methane activators, we have initiated two lines of research: (1) analysis of reaction surfaces for methane activation by prototypical high-valent [9,14k] and low-valent [14j] complexes; (2) investigation of complexes capable of effecting C—H activation by [2 + 2] and oxidative addition [14h]. By understanding what interactions determine the preference for [2 + 2] or oxidative addition in systems for which theory and experiment are in agreement as to the preferred C—H activation mechanisms, we can begin to understand complexes whose activation mechanisms are unclear.

Experimentalists have sought to model reaction coordinates using metric data from related complexes with differing ancillary ligands, an approach termed a Bürgi–Dunitz analysis [55]. Crabtree et al. [56] have constructed a C—H oxidative addition trajectory from crystal structures of agostic complexes. A rigorous theoretical trajectory is provided by the IRC defined as the steepest descent path (in mass-weighted cartesian coordinates) from transition state to reactants and products [57]. Calculation of the IRC reveals a dynamic picture of important interactions affecting methane activation [9]. For example, analysis of IRCs for methane activation by Group IVB imidos clearly shows the importance of agostic interactions in facilitating bond scission (even when not present in ground state products and reactants) [9a], as has been suggested by experimentalists since agostic complexes were first characterized [58]. The IRC for methane activation by oxidative addition of C—H to $Ir(PH_3)_2(H)$ (**9**) was compared with $[2_\sigma + 2_\pi]$ addition to the imido bond of $W(=NH)_3$ (**10**)

$$Ir(PH_3)_2(H) + CH_4 \rightarrow \ddagger_{OA} \rightarrow Ir(PH_3)_2(H)_2(CH_3) \quad (4)$$

$$W(=NH)_3 + CH_4 \rightarrow \ddagger_{[2_\sigma + 2_\pi]} \rightarrow W(=NH)_2(NH_2)(CH_3) \quad (5)$$

Complexes **9** and **10** were chosen because of the similar covalent radii of the TMs, but the results are typical of all IRCs for HX activation investigated to date [9,14g–14j]. The IRCs were calculated using ECP methods on a parallel supercom-

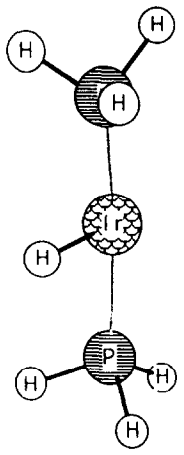

9

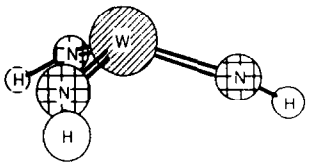

10

puter and the progress of the internal coordinates studied by Crabtree et al. [56] (C—H distance and M—H—C angle) were followed along the IRC; the plot in Fig. 5 is obtained. The transition state is set arbitrarily at $S_{total} = 0$ bohr amu$^{1/2}$ (S_{total} is the mass-weighted distance in cartesians along the IRC). The reactants in Eqs. (4) and (5) have positive S_{total}, while C—H activated products have negative S_{total}. The most obvious feature of Fig. 5 is the similarity of the curves for oxidative and [2 + 2] addition despite differences in the ultimate fate of the activated C—H bond. In both cases, the methane C—H bond remains close to its equilibrium value until the transition state (TS) is imminent. The rapid increase in C—H distance concomitant with a sharp decrease in the M—H—C angle should be noted at $S_{total} \approx 1$ bohr amu$^{1/2}$. Inspection of the Crabtree trajectory [56] shows a rough correlation between a decrease in the M—H—C angle and an increase in C—H distance.

According to the Saillard–Hoffmann model [35], the bonding between C—H bonds and metal centers arises from two synergistic interactions — donation of electron density from σ_{CH} to a vacant metal-based orbital and back donation from a filled metal orbital to σ_{CH}*. If the M/H—C interaction were totally dominated by steric considerations, an M—H—C angle of 180° would be expected; electronic considerations (particularly the need for effective overlap for back donation) dictate an M—H—C angle of less than 90°. The value of M—H—C $\approx$ 105° in the early portion of the activation event is somewhat less than the 130° in the experimental trajectory [56]. Some differences between calculated and experimental trajectories is expected since the experimental trajectory is derived from agostic complexes [56] (i.e. intramolecular C—H/M interactions) which have less freedom to explore conformational space that intermolecular C—H/M interactions. The calculated angle of approach for both high- and low-valent complexes is approximately 105°, suggesting a subtle interplay of steric and electronic factors controlling M/H—C interaction.

The power of computational methods, as applied to reactivity and catalysis, lies

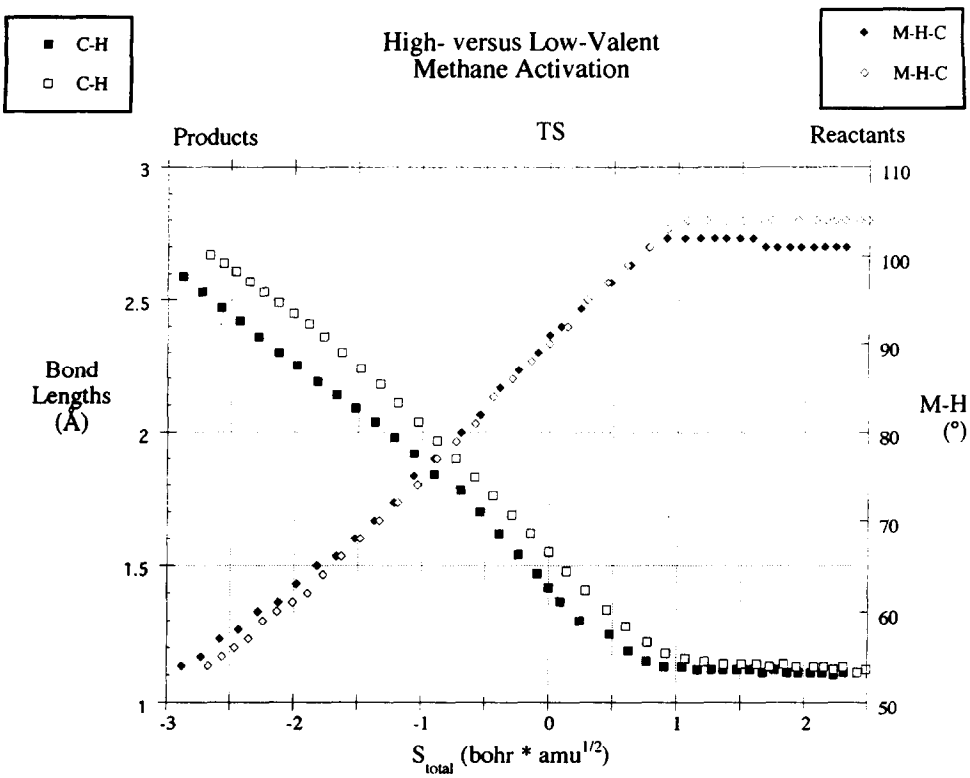

Fig. 5. Changes in C—H distances and M—H—C angles for the C—H bond in methane activated by $Ir(PH)_3(H)$ (open symbols) and $W(=NH)_3$ (filled symbols) as shown in Eqs. (4) and (5).

in their ability to see the "unseen," i.e. reactive intermediates, transition states and points along the IRC, portions of the catalytic cycle for which direct experimental evidence is often limited. Comparison of the IRCs for C—H activation surfaces with the experimental trajectory not only gives confidence in the computational methods (and vice versa), but the computed IRC presents certain advantages: (1) the IRC is for one complex, not a family of complexes as in a Bürgi–Dunitz analysis; (2) points near the transition state can be sampled; (3) theory can provide insight into electronic structural reasons for observed dynamic effects. For example, inspection of the wavefunction along the IRC shows the charge on the methane fragment to increase for both the low- and high-valent complexes from the reactants (a methane adduct) to the "break point" at $S_{total} \approx 1$ bohr amu$^{1/2}$ (Fig. 5). In terms of the Saillard–Hoffmann model [35], donation is increasing relative to back donation — the complex is acting as an electrophile. High-valent complexes are d^0, so we expect electrophilic behavior; the low-valent complex can be considered as electron deficient since it is a 14-electron complex, short of an 18-electron count. Similar arguments can be made for 16-electron C—H activators. After the "break point", the calculated charge on the methane fragment begins to decrease: back donation is increasing

relative to donation and the activating complex is acting as a nucleophile. For low-valent complexes, frontier MOs are dominated by metal-based orbitals, so that both ends of the C—H bond end up on the metal, giving rise to oxidative addition. For high-valent complexes, particularly the multiply bonded complexes focused on to date, frontier MOs are metal–ligand, π bonding MOs (the most plausible source of electron density with which to populate σ_{CH}*) polarized towards the more electronegative MG elements (particularly for MG ≡ C, N, O) leading to [2 + 2] addition. The ECP studies suggest a "two-stage" model of methane activation in which there is similarity in the early part of the reaction coordinate when σ_{CH} donation to a vacant metal-based orbital is dominant ("electrophilic" stage). To cleave the H_3C—H bond, significant population of σ_{CH}* develops from an electron source on the activating complex ("nucleophilic" stage). It is at the moment of decision, when σ_{CH}* must be populated for C—H scission, that oxidative and [2 + 2] addition pathways diverge. An ECP study of methane activation by oxidative and [2 + 2] addition for a d^2 W–imido complex [14j] suggests that this divergence of pathways, at least in an energetic sense, occurs relatively late along the IRC and in the neighborhood of the "break point". Thus the study of this technologically important reaction, feasible only through the use of ECPs, points to greater similarity in two seemingly disparate reactions.

5. Summary

In summary, we have focused on research from our laboratories in order to highlight the utility of effective core potentials for addressing computational problems in coordination chemistry. Our main emphasis to date has been on the development of methods for treating the entire d block [12]. However, research on complexes incorporating the heavier MG elements [14l–o] highlights the utility of ECPs for treating heavier p block elements. Similarly, an ECP approach to the f block metals is a worthy avenue for future research [6c] given the growing interest in these elements. Thus effective core potential methods, particularly when coupled with emerging technologies such as parallel supercomputing, constitute an exciting approach towards the goal of developing methods for addressing the chemistry of the entire Periodic Table.

Acknowledgments

T.R.C. wishes to acknowledge the Petroleum Research Fund (administered by the American Chemical Society), IBM, the National Science Foundation (grant CHE-9314732 and its support of the Cornell National Supercomputer Facility, San Diego Supercomputing Center and National Center for Supercomputing Applications), the Joint Institute for Computational Science (a coalition to encourage high performance computing in Tennessee), the University of Memphis (through Faculty Research Grants), the National Institutes of Standards and Technology and

the Air Force Office of Scientific Research for partial support of ECP studies at the University of Memphis. M.S.G. wishes to acknowledge support from the National Science Foundation (CHE-9313717) and the Air Force Office of Scientific Research (92-0226). T.R.C. and M.S.G. would like to thank the many experimentalists who shared their insight and results with us, most notably Professors Mayer (Washington), Parkin (Columbia), Schrock (MIT), Wigley (Arizona) and Wolczanski (Cornell). Parallelization of GAMESS has advanced greatly through the efforts of Theresa Windus (Northwestern), Mike Schmidt (Iowa State) and Jerry Boatz (Edwards AFB). Finally, none of this work would have been possible without the gracious consent of Stevens, Basch, Krauss and Jasien to incorporate their ECP scheme into GAMESS.

References

[1] F.A. Cotton and G. Wilkinson, Advanced Inorganic Chemistry, Wiley, New York, 5th edn., 1988.
[2] (a) M.C. Zerner and D. Salahub, The Challenge of d- and f-Electrons, ACS, Washington DC, 1989.
(b) A. Veillard (ed.), Quantum Chemistry: The Challenge of Transition Metals and Coordination Chemistry, Reidel, Dordrecht, 1985.
[3] (a) R. Boca and P. Pelikan, Coord. Chem. Rev., 118 (1992) 1.
(b) Z. Lin and M.B. Hall, Coord. Chem. Rev., 123 (1993) 149.
[4] W.J. Hehre, L. Radom, P.v.R. Schleyer and J.A. Pople, Ab-Initio Molecular Orbital Theory, Wiley, New York, 1986.
[5] Recent articles on the approaches to computational d and f block chemistry can be found in: T. Ziegler, Chem. Rev., 91 (1991) 649–1108.
[6] (a) M. Krauss, W.J. Stevens, H. Basch and P.G. Jasien, Can. J. Chem., 70 (1992) 612.
(b) W.J. Stevens, H. Basch and M. Krauss, J. Chem. Phys., 81 (1984) 6026.
(c) T.R. Cundari and W.J. Stevens, J. Chem. Phys., 98 (1993) 5555.
(d) P.J. Hay and W.R. Wadt, J. Chem. Phys., 82 (1985) 270, 284, 299.
(e) M.M. Hurley, L.F. Pacios, P.A. Christiansen, R.B. Ross and W.C. Ermler, J. Chem. Phys., 84 (1986) 6640; L.A. La John, P.A. Christiansen, R.B. Ross, T. Atashroo and W.C. Ermler, J. Am. Chem. Soc., 87 (1987) 2812.
(f) M. Dolg and H. Stoll, Theor. Chim. Acta, 75 (1989) 369; M. Dolg, H. Stoll and H. Preuss, J. Chem. Phys., 90 (1989) 1730.
[7] (a) GAMESS: M.W. Schmidt, K.K. Baldridge, J.A. Boatz, J.H. Jensen, S. Koseki, M.S. Gordon, K.A. Nguyen, T.L. Windus and S.T. Elbert, QCPE Bulletin, 10 (1990) 52.
(b) Details concerning the parallel implementation of GAMESS are given in: M.W. Schmidt, K.K. Baldridge, J.A. Boatz, J.H. Jensen, S. Koseki, N. Matsunaga, M.S. Gordon, K.A. Nguyen, S. Su, T.L. Windus, S.T. Elbert, J. Montgomery and M. Dupuis, J. Comp. Chem., 14 (1993) 1347.
[8] P. Carsky, B.A. Hess and L.J. Schaad, J. Comp. Chem., 5 (1984) 280.
[9] (a) T.R. Cundari, J. Am. Chem. Soc., 114 (1992) 10 557.
(b) T.R. Cundari, Organometallics, submitted for publication.
[10] (a) H.J. Werner and P.J. Knowles, J. Chem. Phys., 89 (1988) 5803.
(b) H.J. Werner and P.J. Knowles, Chem. Phys. Lett., 145 (1988) 514.
[11] (a) K. Anderson, P.A. Malmquist and B.O. Roos, J. Chem. Phys., 96 (1992) 1218.
(b) K. Anderson, P.A. Malmquist and B.O. Roos, J. Phys. Chem., 94 (1990) 5483.
[12] W.A. Nugent and J.M. Mayer, Metal–Ligand Multiple Bonds, Wiley, New York, 1988.
[13] TM=phosphinidene complexes:
(a) A.H. Cowley and A.R. Barron, Acc. Chem. Res., 21 (1988) 81.
(b) P.B. Hitchcock, M.F. Lappert and W.P. Leung, J. Chem. Soc. Chem. Commun., (1987) 1282.
(c) R.R. Schrock, C.C. Cummins and W.M. Davis, Angew. Chem., Int. Ed. Engl., 32 (1993) 756.
(d) D.W. Stephan, Z. Hou and T.C. Breen, Organometallics, 12 (1993) 3158.

TM = chalcogen complexes:
(e) G. Parkin and W.A. Howard, J. Am. Chem. Soc., accepted for publication.
(f) V. Christou and J. Arnold, J. Am. Chem. Soc., 114 (1992) 6240.
(g) E. Diemann and A. Müller, Coord. Chem. Rev., 10 (1973) 79.
TM = tetralide complexes:
(h) W. Petz, Chem. Rev., 86 (1986) 1019.
(i) W.A. Herrmann, Angew. Chem., Int. Ed. Engl., 25 (1986) 56.

[14] To date, effective core potential studies of alkylidene [14a–c], silylidene [14d,e], imido [9,14f–k], phosphinidene [14l,m] and chalcogenido [14n,o] complexes have been reported from our laboratories.
(a) T.R. Cundari and M.S. Gordon, J. Am. Chem. Soc., 113 (1991) 5231.
(b) T.R. Cundari and M.S. Gordon, Organometallics, 11 (1992) 55.
(c) T.R. Cundari and M.S. Gordon, J. Am. Chem. Soc., 114 (1992) 539.
(d) T.R. Cundari and M.S. Gordon, J. Phys. Chem., 96 (1992) 631.
(e) T.R. Cundari and M.S. Gordon, Organometallics, 11 (1992) 3122.
(f) T.R. Cundari, J. Am. Chem. Soc., 114 (1992) 7879.
(g) T.R. Cundari, Int. J. Quantum Chem., Proc. Sanibel Symp., 26 (1992) 793.
(h) T.R. Cundari, Organometallics, 12 (1993) 4971.
(i) T.R. Cundari and M.S. Gordon, J. Am. Chem. Soc., 115 (1993) 4210.
(j) T.R. Cundari, J. Am. Chem. Soc., 116 (1994) 340.
(k) T.R. Cundari, Organometallics, 12 (1993) 1998.
(l) T.R. Cundari, M.S. Gordon and K. Takano, unpublished results, 1994.
(m) M.T. Benson, T.R. Cundari, Y. Li and L.A. Strohecker, Int. J. Quantum Chem., Proc. Sanibel Symp., accepted for publication.
(n) T.R. Cundari, S.C. Critchlow, R.R. Conry, E. Spaltenstein, K.A. Hall, S. Tahmassebi and J.M. Mayer, Organometallics, 13 (1994) 322.
(o) M.T. Benson, T.R. Cundari, S.J. Lim, H. Nguyen and K. Pierce-Beaver, J. Am. Chem. Soc., accepted for publication.

[15] (a) R.R. Schrock, Acc. Chem. Res., 23 (1990) 158.
(b) R. Toreki, R.R. Schrock and W.M. Davis, J. Am. Chem. Soc., 114 (1992) 3367; R. Toreki, G.A. Vaughan, R.R. Schrock and W.M. Davis, J. Am. Chem. Soc., 115 (1993) 127.

[16] F.A. Cotton and G. Wilkinson, Advanced Inorganic Chemistry, Wiley, New York, 5th edn., 1988, p. 1108.

[17] G. Wilkinson, A.D. Danopoulos, T. Sweet and M.B. Hursthouse, J. Chem. Soc. Chem. Commun., (1993) 495.

[18] J.C. Bryan and A.K. Burrell, Angew. Chem., Int. Ed. Engl., 32 (1993) 94.

[19] T.L. Windus, M.W. Schmidt and M.S. Gordon, Theor. Chim. Acta, in press.

[20] M.R. Smith, P.T. Matsunaga and R.A. Andersen, J. Am. Chem. Soc., 115 (1993) 7049.

[21] (a) M.B. Hall and T.E. Taylor, J. Am. Chem. Soc., 106 (1984) 1576.
(b) J.P. Collmann, L.S. Hegedus, J.R. Norton and R.G. Finke, Principles and Applications of Organotransition Metal Chemistry, University Science Books, Mills Valley, 1987.
(c) R.R. Schrock, J. Am. Chem. Soc., 98 (1976) 5399.
(d) C.P. Casey and S.W. Polichowski, J. Am. Chem. Soc., 99 (1977) 6097.
(e) C.P. Casey and H.J. Tuinstra, J. Am. Chem. Soc., 100 (1978) 2270.
(f) M. Brookhart and W.R. Studabaker, Chem. Rev., 87 (1987) 411.
(g) P. Gassmann and T.J. Johnson, J. Am. Chem. Soc., 99 (1977) 622.
(h) M. Brookhart, M.B. Humphrey, H.J. Kratzer and G.O. Nelson, J. Am. Chem. Soc., 102 (1980) 7802.
(i) H.E. Ardill, R.M.E. Greene, J.G. Hamilton, H.T. Ho, K.J. Ivin, J.G. Lapienis, G.M. McCann and J.J. Ronney, in J.E. McGrath (ed.), Ring Opening Polymerization, American Chemical Society, Washington DC, 1985, p. 285.

[22] Caution must be exercised in inferring bonding descriptions from structural data [14f]. For example, Parkin et al. [22a] have reported $Cp^*_2Ta(NPh)(H)$ which shows a longer than normal Ta–imido bond, 1.831(1) Å, despite near-perfect linear coordination (usually taken to infer a

metal–imido triple bond) of the imido ligand. Gray et al. [22b] report a four-coordinate Ta–imido with a very small $Ta-N_{imido}-C$ angle of 145.7(6)° (usually taken to infer a metal–imido double bond) which displays a Ta–imido bond length, 1.779(8) Å, consistent with the four-coordinate, linear Ta(V)–imidos reported in the compendium of Nugent and Mayer [12] (1.77 ± 0.01 Å).
(a) G. Parkin, A. van Asselt, D.J. Leahy, L. Whinnery, N.G. Hua, R.W. Quan, L.M. Henling, W.P. Schaefer, B.D. Santarsiero and J.E. Bercaw, Inorg. Chem., 31 (1992) 82.
(b) S.D. Gray, D.P. Smith, M.A. Bruck and D.E. Wigley, J. Am. Chem. Soc., 114 (1992) 5426.
[23] D.L. Cooper, J. Gerratt and M. Raimondi, Adv. Chem. Phys., 27 (1987) (Part II) 319.
[24] T.L. Windus and M.S. Gordon, J. Am. Chem. Soc., 114 (1992) 9559.
[25] W.A. Nugent, R.J. McKinney, R.V. Kasowski and F.A. Van-Catledge, Inorg. Chim. Acta, 65 (1982) L91.
[26] An interesting discussion of the methane conversion problem from the industrial point of view is given in: N.D. Parkyns, Chem. Br., 9 (1990) 841.
[27] Overviews of hydrocarbon C—H activation can be found in:
(a) C.L. Hill (ed.), Activation and Functionalization of Alkanes, Wiley, New York, 1988.
(b) J.A. Davies (ed.), Selective Hydrocarbon Activation, VCH, New York, 1990.
[28] (a) A.M. Khenkin and A.E. Shilov, New. J. Chem., 13 (1989) 659.
(b) P.R. Ortiz de Montellano (ed.), Cytochrome P-450, Plenum, New York, 1986.
[29] G.A. Olah, Acc. Chem. Res., 20 (1987) 422.
[30] I.P. Rothwell, in C.L. Hill (ed.), Activation and Functionalization of Alkanes, Wiley, New York, 1988, p. 151.
[31] P.L. Watson, in J.A. Davies (ed.), Selective Hydrocarbon Activation, VCH, New York, 1990, p. 79.
[32] (a) C.C. Cummins, S.M. Baxter and P.T. Wolczanski, Methane activation by Zr–imido, J. Am. Chem. Soc., 110 (1988) 8731.
(b) C.P. Schaller and P.T. Wolczanski, Methane activation by Ta–bis(imido), Inorg. Chem., 32 (1993) 131.
(c) J. de With and A.D. Horton, Methane activation by V–bis(imido), Angew. Chem., Int. Ed. Engl., 32 (1993) 903.
(d) P.T. Wolczanski, Methane activation by Ti–imido, (Cornell), personal communication, 1994.
[33] C.M. Fendrick and T.J. Marks, J. Am. Chem. Soc., 106 (1984) 2214.
[34] W.D. Jones, in C.L. Hill (ed.), Activation and Functionalization of Alkanes, Wiley, New York, 1988, p. 111.
[35] J.Y. Saillard and R. Hoffmann, J. Am. Chem. Soc., 106 (1984) 2006.
[36] A.H. Janowicz and R.G. Bergman, J. Am. Chem. Soc., 104 (1982) 352.
[37] J.K. Hoyano and W.A.G. Graham, J. Am. Chem. Soc., 104 (1982) 3723.
[38] W.D. Jones and F.J. Feher, J. Am. Chem. Soc., 104 (1982) 4240.
[39] M.J. Burk and R.H. Crabtree, J. Am. Chem. Soc., 109 (1987) 8025.
[40] C.J. Cameron, H. Felkin, T. Fillebeen-Khan, N.J. Forrow and E. Guittet, J. Chem. Soc., Chem. Commun., (1986) 801.
[41] T. Sakakura and M. Tanaka, Chem. Lett., 249 (1987) 1113; T. Sakakura and M. Tanaka, J. Chem. Soc., Chem. Commun., (1987) 758.
[42] M. Schulz and H. Werner, Organometallics, 11 (1992) 2790.
[43] The study of gas phase reactions between atomic transition metal ions and alkanes is documented in: P.B. Armentrout and J.L. Beauchamp, Acc. Chem. Res., 22 (1989) 315 and P.B. Armentrout in D.H. Russell (ed.), Gas Phase Inorganic Chemistry, Plenum, New York, 1989.
[44] D.G. Musaev, K. Morokuma, N. Koga, K.A. Nguyen, M.S. Gordon and T.R. Cundari, J. Phys. Chem., 97 (1993) 11435.
[45] P.R. Kemper, J. Bushnell, P. van Koppen and M.T. Bowers, J. Phys. Chem., 97 (1993) 1810.
[46] P.B. Armentrout, L.E. Sunderlin and E.R. Fisher, Inorg. Chem., 28 (1989) 4436.
[47] R.L. Hettich and B.S. Freiser, J. Am. Chem. Soc., 108 (1986) 2537.
[48] P.R. Kemper and M.T. Bowers, J. Am. Soc. Mass Spectrom., 1 (1990) 197.
[49] A.E. Shilov, Activation of Saturated Hydrocarbons, Reidel, Boston, 1984.
[50] A. Sen, Acc. Chem. Res., 21 (1988) 421.
[51] A. Sen, M. Lin, L.C. Kao and A.C. Hutson, J. Am. Chem. Soc., 114 (1992) 6385.

[52] J.E. Bercaw, J.A. Labinger and A.M. Herring, J. Am. Chem. Soc., 112 (1990) 5628.
[53] J.E. Bercaw, J.A. Labinger, A.M. Herring, D.K. Lyon, G.A. Luinstra, I.T. Horváth and K. Eller, Organometallics, 12 (1993) 895.
[54] R.A. Periana, D.J. Taube, E.R. Evitt, D.G. Löffler, P.R. Wentrcek, G Voss and T. Masuda, Science, 259 (1993) 340.
[55] H.B. Bürgi and J.D. Dunitz, Acc. Chem. Res., 16 (1983) 153.
[56] R.H. Crabtree, E.M. Holt, M. Lavin and S.M. Morehouse, Inorg. Chem., 24 (1985) 1986.
[57] Intrinsic reaction coordinates were calculated using the algorithm described in: C. Gonzalez and H.B. Schlegel, J. Chem. Phys., 90 (1989) 2154.
[58] M.L.H. Green, M. Brookhart and L.K. Wong, Prog. Inorg. Chem., 36 (1988) 1.